Requirement for p38 and p44/p42 Mitogen-Activated Protein Kinases in RAGE-Mediated Nuclear Factor-κB Transcriptional Activation and Cytokine Secretion

Chen-Hsiung Yeh,[1] Lydia Sturgis,[1] Joe Haidacher,[1] Xue-Nong Zhang,[1] Sidney J. Sherwood,[1] Robert J. Bjercke,[2] Ondrej Juhasz,[3] Michael T. Crow,[3] Ronald G. Tilton,[1] and Larry Denner[1]

Advanced glycation end product (AGE) activation of the signal-transducing receptor for AGE (RAGE) has been linked to a proinflammatory phenotypic change within cells. However, the precise intracellular signaling pathways involved have not been elucidated. We demonstrate here that human serum albumin modified with N^{ε}-(carboxymethyl)lysine (CML), a major AGE adduct that progressively accumulates with aging, diabetes, and renal failure, induced nuclear factor (NF)-κB–driven reporter gene expression in human monocytic THP-1 cells. The NF-κB response was blocked with a synthetic peptide corresponding to the putative ligand-binding domain of RAGE, with anti-RAGE antiserum, and by coexpression of truncated receptors lacking the intracellular domain. Signal transduction from RAGE to NF-κB involved the generation of reactive oxygen species, since reporter gene expression was blocked with the antioxidant *N*-acetyl-L-cysteine. CML-modified albumin produced rapid transient activation of tyrosine phosphorylation, extracellular signal-regulated kinase 1 and 2, and p38 mitogen-activated protein kinase (MAPK), but not c-Jun NH_2-terminal kinase. RAGE-mediated NF-κB activation was suppressed by the selective p38 MAPK inhibitor SB203580 and by coexpression of a kinase-dead p38 dominant-negative mutant. Activation of NF-κB by CML-modified albumin increased secretion of proinflammatory cytokines (tumor necrosis factor-α, interleukin-1β, and monocyte chemoattractant protein-1) severalfold, and inhibition of p38 MAPK blocked these increases. These results indicate that p38 MAPK activation mediates RAGE-induced NF-κB–dependent secretion of proinflammatory cytokines and suggest that accelerated inflammation may be a consequence of cellular activation induced by this receptor. *Diabetes* 50:1495–1504, 2001

From the Department of [1]Cell Biology and Apoptosis Program and the [2]Department of Immunology, Texas Biotechnology Corporation, Houston, Texas; and the [3]Laboratory of Cardiovascular Science, National Institute on Aging, National Institutes of Health, Baltimore, Maryland.

Address correspondence and reprint requests to Dr. Larry Denner, PhD, Department of Cell Biology, Texas Biotechnology Corporation, 7000 Fannin, Houston, TX 77030. E-mail: ldenner@tbc.com.

Received for publication 7 July 2000 and accepted in revised form 15 March 2001.

C.-H.Y., L.S., J.H., X.-N.Z., S.J.S., R.J.B., R.G.T., and L.D. are stock shareholders.

CML-HSA, N^{ε}-(carboxymethyl)lysine; DTT, dithiothreitol; ELISA, enzyme-linked immunosorbent assay; ERK, extracellular signal-regulated kinase; HSA, human serum albumin; IL, interleukin; JNK, c-Jun NH_2-terminal kinase; MAPK, mitogen-activated protein kinase; MCP, monocyte chemoattractant protein; NAC, *N*-acetyl-L-cysteine; NF, nuclear factor; PCR, polymerase chain reaction; PMSF, phenylmethylsulfonyl fluoride; PTK, protein tyrosine kinase; RAGE, receptor for AGE; RT, reverse transcriptase; SFM, serum-free medium; TNF, tumor necrosis factor.

Glucose and other reducing sugars can react nonenzymatically with amino groups of proteins and lipids to form Schiff bases that, through multiple rearrangements, are transformed into irreversibly cross-linked fluorescent advanced glycation end products (AGEs) (1–3). The formation and accumulation of AGE adducts in various tissues are known to progress as a function of age and glycemia, are associated with altered protein structure and function, and are able to generate reactive oxygen intermediates and induce cellular activation and inflammation (1,4). Accumulation of AGEs has been implicated in the pathogenesis of numerous diverse disorders, including diabetes (1,5), Alzheimer's disease (6,7), and hemodialysis-associated amyloidosis (8), as well as the natural aging process (1,9). The finding that pharmacological inhibition of AGE formation prevents vascular complications affecting retina, kidney, and nerves in long-term diabetic animals provides support for this suggestion (1,10,11).

One mechanism by which AGEs exert their effects on cellular function is via interaction with specific receptors. Several AGE-binding proteins have been identified, including lactoferrin (12), oligosaccharyl transferase complex protein 48 (AGE-R1) (13,14), 80K-H protein (AGE-R2) (13,14), galectin-3 (AGE-R3) (15), lysozyme (16), and the receptor for AGE (RAGE) (12,17). RAGE is a multiligand member of the immunoglobulin superfamily and is expressed on the surface of a variety of cell types, including endothelial cells, smooth muscle cells, lymphocytes, monocytes, and neurons (18,19). Increased RAGE expression has been shown in both endothelium and vascular smooth muscle cells from diabetic patients (5,20) and in macrophages from patients with renal failure and dialysis-related amyloidosis (21). Areas of enhanced RAGE immunoreactivity colocalize with immunostaining for AGE-reactive epitopes. Recent studies also have demonstrated elevated RAGE expression in affected neurons in Alzheimer's disease (7) and in vasculatures affected by autoimmune/inflammatory disorders (6). Interruption of AGE-RAGE interaction by administration of the soluble extracellular domain of RAGE has been shown to suppress diabetes-induced vascular hyperpermeability (22) and the accelerated development of atherosclerosis in diabetic apolipoprotein E knockout mice (23). Although these findings support a causal role for RAGE in the pathogenesis of

Downloaded from http://diabetesjournals.org/diabetes/article-pdf/50/6/1495/654502/1495.pdf by guest on 04 December 2023

diabetes-induced vascular functional and structural changes, the intracellular mechanisms by which AGE-RAGE interaction causes vascular dysfunction remain unclear.

Interaction of AGE with RAGE has been shown to generate an oxidative stress that results in activation of nuclear factor (NF)-κB, the oxidant-sensitive transcription factor (24). NF-κB may contribute to the development of a proinflammatory state by stimulating expression of target genes, such as heme oxygenase (25), vascular cell adhesion molecule-1 (VCAM-1) (26), procoagulant tissue factor (27), endothelin-1 (28), macrophage colony–stimulating factor (24), and RAGE itself (29). Despite these observations, information regarding signal transduction from RAGE to NF-κB–induced cytokine secretion remains largely unknown. Several reports have linked reactive oxygen species (24), p21Ras, and extracellular signal-regulated kinase (ERK) 1 and 2 (30) to this signaling pathway, yet the potential role of other relevant signaling molecules remains unknown.

The purpose of the present study was to elucidate intracellular signaling pathways linked to RAGE activation in monocytes using the ligand N^{ϵ}-(carboxymethyl)lysine (CML)-modified human serum albumin (HSA). CML is a major adduct of AGE-modified proteins that accumulates in diabetic patients, has been recognized as a marker of oxidative stress (31,32), and recently has been demonstrated to be a ligand for RAGE (33). We identified p38 mitogen-activated protein kinase (MAPK) as a key downstream effector of RAGE, since p38 is required for CML-HSA–induced NF-κB transcriptional activation and the subsequent increased secretion of tumor necrosis factor (TNF)-α, interleukin (IL)-1β, and monocyte chemoattractant protein (MCP)-1. This report establishes a RAGE–p38 MAPK –NF-κB– cytokine signaling cascade in monocytes and raises the possibility that it may have physiological importance in the development of the proinflammatory milieu associated with such diverse diseases as Alzheimer's, atherosclerosis, and diabetes.

RESEARCH DESIGN AND METHODS

Materials. All tissue culture reagents were purchased from Life Technologies and were documented to be free of endotoxins. HSA (Fraction V), glyoxylic acid, and sodium cyanoborohydride were obtained from Sigma (St. Louis, MO). *N*-acetyl-L-cysteine (NAC), genistein, PD98059, and SB203580 were from Calbiochem (San Diego, CA). Anti-phosphotyrosine antibody (PY99) was from Santa Cruz Biotechnology (Santa Cruz, CA). Anti-ERK1/2, anti–phospho-ERK1/2, anti-p38, anti–phospho-p38, anti–c-Jun NH_2-terminal kinase (JNK), anti–phospho-JNK, and anti–phospho-ATF2 antibodies were purchased from New England BioLabs (Beverly, MA). Synthetic peptides were prepared by Dr. Kaijun Ren (Chemistry Department, Texas Biotechnology Corporation) and were >95% pure, as assessed by high-performance liquid chromatography. The expression plasmid for the p38 kinase-dead dominant-negative mutant was provided by Dr. Roger Davis from the Howard Hughes Medical Institute at the University of Massachusetts Medical Center (Worcester, MA). The IκB mutant was a gift from Dr. Chung Y. Hsu at Washington University School of Medicine (St. Louis, MO). Both mutants are in the pcDNA3.1 expression vector. Enzyme-linked immunosorbent assay (ELISA) kits for TNF-α, IL-1β, and MCP-1 were from R&D Systems (Minneapolis, MN).

Preparation of CML-HSA. CML-HSA was prepared as previously described (34). Briefly, 175 mg/ml HSA was incubated at 37°C for 24 h in 0.2 mol/l sodium phosphate buffer (pH 7.8) containing 150 mmol/l glyoxylic acid and 450 mmol/l sodium cyanoborohydride, followed by extensive dialysis against 2 L phospate-buffered saline at 4°C changed twice at 24-h intervals. The resulting CML-HSA preparation contained ~30% CML-modified lysine residues per molecule albumin based on amino acid analysis. Both the CML-HSA and the control HSA were documented to be endotoxin-free by use of the Limulus amebocyte lysate assay (Sigma E-TOXATE). The lower limits of detection were 0.015 EU/ml (turbid gel), 0.03 EU/ml (soft gel), and 0.06 EU/ml (hard gel).

Cell culture. Human THP-1 monocytic leukemia cells were obtained from the American *Type Culture* Collection (ATCC TIB-202; Rockville, MD) and maintained in RPMI 1640 medium supplemented with 10% fetal bovine serum, 50 μmol/l 2-mercaptoethanol, 2 mmol/l glutamine, 100 U penicillin, and 100 μg/ml streptomycin. Cells were grown at 37°C in a 5% CO_2 atmosphere. Log-phase cells were used for all experiments.

Human peripheral monocytes were isolated from healthy donors' blood (SeraCare, Oceanside, CA) using standard Ficoll-Hypaque (Amersham Pharmacia Biotech, Uppsala, Sweden) density-gradient centrifugation followed by adherence depletion of lymphocytes as previously described (35). Cells were seeded at 4×10^5 cells per well in a 48-well plate and treated with 100 μg/ml HSA or CML-HSA in the absence or presence of SB203580 or PD98059 for 24 h before measurement of TNF-α in the culture media by ELISA.

Anti-RAGE antiserum preparation. The human RAGE extracellular domain encompassing residues 23–340 (sRAGE) was expressed and purified from *Escherichia coli* using the pET thioredoxin system (Novagen, Madison, WI). For antiserum production, BALB/c mice were immunized with 100 μg sRAGE protein in complete Freund's adjuvant, and an additional 50 μg sRAGE in incomplete Freund's adjuvant was given every 4 weeks until a high serum titer was achieved. NF-κB reporter neutralizing activity of the antiserum was measured by preincubation with THP-1 cells (1:5 or 1:25 dilution of the antiserum) for 1 h before exposure to CML-HSA.

DEAE/dextran-mediated cell transfection and luciferase assay. THP-1 cells were seeded at 5×10^6 cells per 100-mm dish in 10 ml of serum-free medium (SFM) the day before transfection. Transfection was performed by the DEAE-dextran method as described previously (36), with minor modifications. Cells were washed once with SFM and resuspended in 1 ml of the same medium containing 2 μg NF-κB–Luc reporter plasmid (Clontech, Palo Alto, CA) and 200 μg/ml DEAE-dextran (Promega, Madison, WI). The cell-DNA mixture was incubated at room temperature for 20–30 min before washing, centrifugation, and resuspension into fresh SFM. Transfected cells were seeded into 96-well plates at 70,000 cells per well for recovery. After 24 h, cells were treated with the indicated amount of control albumin or CML-modified albumin for 10 min to 24 h before cell harvest. Equivalent amounts of cell lysates, normalized for total protein (Bradford protein assay; Bio-Rad, Palo Alto, CA), were used for measurement of luciferase activity. Luciferase assays were performed using the Steady-Glo luciferase assay system according to the manufacturer's instructions (Promega), and luminescence was detected in a TopCount microplate scintillation counter, using a single-photon monitor program (Packard Instrument Company, Meriden, CT). For cotransfection experiments, 10 μg (10-fold molar excess) of expression plasmid was used with 1 μg of the NF-κB reporter, with the empty vector serving as a transfection control. Transfection efficiency in THP-1 cells was 20–30%, as monitored by cotransfection with a β-galactosidase expression plasmid (Clontech).

Electrophoretic mobility shift assay. Cell extracts were prepared using the protocol of Schreiber et al. (37), with minor modifications. Briefly, $2–4 \times 10^6$ cells were collected by centrifugation, washed in Tris-buffered saline, then resuspended by gentle pipetting in 400 μl cold buffer containing 10 mmol/l HEPES, pH 7.9, 10 mmol/l KCl, 0.1 mmol/l EDTA, 0.1 mmol/l EGTA, 1 mmol/l dithiothreitol (DTT), and 0.5 mmol/l phenylmethylsulfonyl fluoride (PMSF). The cell suspension was incubated on ice for 15 min, after which Nonidet-P40 was added to a final concentration of 1%. The homogenate was subjected to centrifugation for 10 s; the pellet was resuspended in 50 μl ice-cold buffer containing 20 mmol/l HEPES, pH 7.9, 0.4 mol/l NaCl, 1 mmol/l EDTA, 1 mmol/l EGTA, 1 mmol/l DTT, and 1 mmol/l PMSF; and the tube was rocked at 4°C for 30 min on a shaking platform then dialyzed against reaction buffer (20 mmol/l HEPES, pH 7.9, 20% glycerol, 50 mmol/l KCl, 0.2 mmol/l EDTA, 1 mmol/l $MgCl_2$, and 1 mmol/l DTT). The nuclear extract was spun for 5 min in the cold room. Total protein content of the supernatant was determined, with the remainder stored at −70°C in aliquots. Some 5 μg of the nuclear extract was mixed with 2 μg poly dI-dC and ~200 pg (10,000 cpm) of radiolabeled double-stranded oligonucleotides containing the c-*myc* NF-κB binding site (CGTT*GGGAAAACCC*GGGATT) in reaction buffer to a final volume of 30 μl and incubated at room temperature for 25 min. Samples were run on a 5% (30:1) polyacrylamide gel in 0.5× Tris-borate-EDTA buffer.

Radiolabeled probes were prepared by labeling one of the oligonucleotides comprising the DNA binding site and then annealing it to its unlabeled partner. Radiolabeling was performed using T4 polynucleotide kinase and [γ-^{32}P]ATP. After this reaction, unincorporated nucleotides and the T4 kinase buffer were removed, the unlabeled oligonucleotide was added, and it was heated to 80°C and then allowed to cool slowly to room temperature.

RAGE-expression plasmids. A cDNA-encoding RAGE was generated by reverse transcriptase (RT)–polymerase chain reaction (PCR) using human lung mRNA as a source for the cDNA and primers based on the published full-length sequence (GenBank AF001095). The product was fully sequenced and then subcloned into the eucaryotic expression vector pcDNA3.1($^+$)neo.

Downloaded from http://diabetesjournals.org/diabetes/article-pdf/50/6/1495/654502/1495.pdf by guest on 04 December 2023

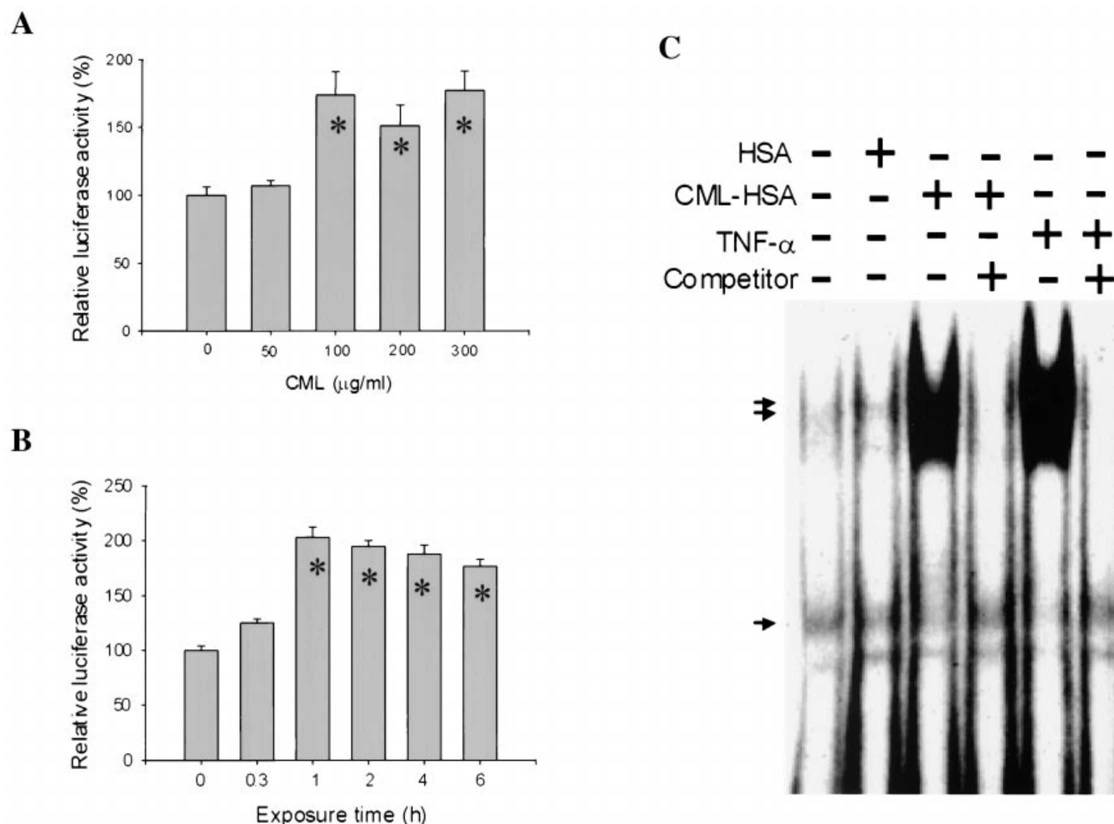

FIG. 1. CML-HSA induces NF-κB transcriptional activation in THP-1 cells. *A*: Concentration-dependent stimulation of NF-κB–luciferase reporter by CML-HSA. THP-1 cells were transiently transfected with the NF-κB–Luc reporter gene, treated 1 h with the indicated concentrations of CML-HSA, and harvested for analysis of luciferase activity. *B*: Time-dependent stimulation of NF-κB–luciferase reporter by CML-HSA. After transfection, cells were exposed to 100 μg/ml CML-HSA for the indicated period of time followed by luciferase measurement. Relative luciferase activities are expressed as the mean ± SE of at least three independent experiments with triplicate determinations, setting the basal (i.e., no CML-HSA exposure) at 100%. *C*: CML-HSA treatment resulted in increased NF-κB DNA-binding activity. Some 5 μg of nuclear extract prepared from THP-1 cells treated for 4 h with 100 μg/ml HSA, 100 μg/ml CML-HSA, or 10 ng/ml recombinant human TNF-α was incubated with radiolabeled double-stranded oligonucleotides containing the c-*myc* NF-κB binding site in the presence or absence of excess unlabeled probe (competitor). The single arrow indicates nonspecific binding to the probe, and the double arrows indicate specific DNA binding that is effectively competed by adding excess unlabeled double-stranded probe or is absent when the binding site was altered (data not shown). *$P < 0.05$ compared with basal levels.

Downloaded from http://diabetesjournals.org/diabetes/article-pdf/50/6/1495/654502/1495.pdf by guest on 04 December 2023

RAGE lacking its intracellular domain was constructed by PCR-based site-directed mutagenesis using primers to introduce a termination codon immediately after amino acid 364 (RAGE-365t) or amino acid 371 (RAGE-372t). RAGE-365t terminates two amino acids after the hydrophobic region thought to be the transmembrane domain, whereas RAGE-372t retains only a portion of the cytosolic tail that is not well conserved across species.

Western blotting analysis. THP-1 monocytes (5×10^6) were solubilized in a lysis buffer containing 50 mmol/l Tris-HCl, pH 7.5, 150 mmol/l NaCl, 1% Nonidet-P40, 0.5% sodium deoxycholate, and protease inhibitor cocktail (Boehringer Mannheim, Indianapolis, IN). Cellular lysates (50 μg) were fractionated on SDS-PAGE and analyzed by immunoblotting. Western blotting was performed using the indicated primary antibodies according to the instructions of each manufacturer. Blots were then stained with the corresponding anti–rabbit or anti–mouse IgG–horseradish-peroxidase conjugate (1:3,000 dilution) and detected by enhanced chemiluminescence reagent (ECL; Amersham, Arlington Heights, IL). Autoradiography was done at room temperature, and the appropriate exposures were quantitated by densitometry.

Measurement of cytokine secretion. ELISA was used for quantitative measurement of released TNF-α, IL-1β, and MCP-1. After treatment of the cells, the media was collected and analyzed by ELISA according to each protocol provided by the manufacturer (R&D Systems).

Statistical analysis. Quantitative data were expressed as means ± SE, based on at least three separate experiments. Unpaired Student's *t* test was used to determine the significance of differences among treatments. A *P* value <0.05 was considered significant.

RESULTS

CML-HSA activates NF-κB transcriptional activity in monocytic THP-1 cells. AGEs have been shown to stimulate NF-κB DNA-binding activity in vitro in a number of cell types (24,26,30,33). To determine whether CML-HSA induces NF-κB transcriptional activity, we used the THP-1 monocytic cell line transiently transfected with an NF-κB reporter gene. Both RT-PCR and Western blot were used to demonstrate the presence of RAGE mRNA and protein, respectively, within THP-1 cells (data not shown). Transfected cells incubated with native HSA or without CML-HSA treatment were used as controls for basal luciferase activity. Treatment with CML-HSA at >100 μg/ml stimulated reporter gene expression by ~1.7-fold as compared with the basal level (Fig. 1*A*). CML-HSA exposure initiated a fast and statistically significant NF-κB response, with an initial induction observed as early as 20 min after treatment. Luciferase activity was elevated approximately two-fold within the first hour and remained essentially unchanged for 24 h (Fig. 1*B*). The lack of further luciferase accumulation after 1 h suggests an acute activation and deactivation of NF-κB, whereas the prolonged signal probably reflects the stability of the luciferase protein. The effect of 10, 5, and 1% CML modification of HSA was tested using the NF-κB reporter assay, and a similar 1.5- to 1.7-fold increase in the luciferase signal was observed at modifications of ≥5% (data not shown).

Nuclear extracts from THP cells treated with either TNF-α or CML-HSA showed a large increase in specific

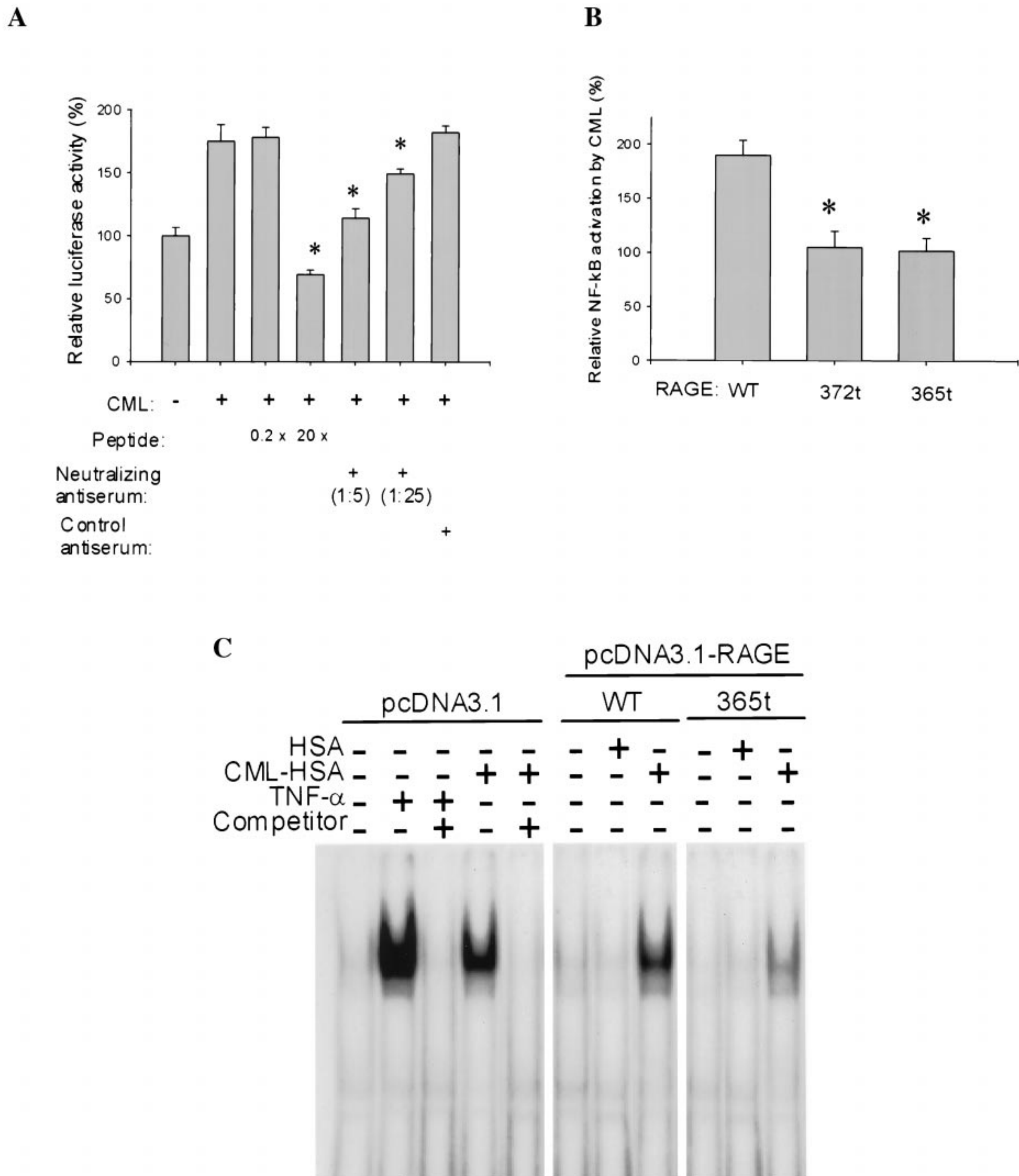

FIG. 2. Requirement for RAGE in the CML-HSA–induced NF-κB response. Blockade of CML-HSA–mediated NF-κB transcriptional activation by a synthetic peptide and neutralizing antiserum (*A*) or by coexpression of RAGE truncation mutants (*B*). *A*: 100 μg/ml CML-HSA was preincubated with or without a synthetic peptide derived from the extracellular ligand-binding domain of RAGE at 37°C for 1 h. The mixtures were then added to cell cultures and incubated for another 1 h before analysis of luciferase activity. For the neutralizing antiserum experiments, RAGE antiserum (at 1:5 and 1:25 dilution) or the preimmune control serum (1:5) were preincubated with the transfected cells for 1 h before CML-HSA stimulation. Results from native HSA treatment were set at 100%. *B*: Full-length (wild-type) RAGE or the cytoplasmic tail truncation mutants RAGE-372t or RAGE-365t were cotransfected with the NF-κB reporter into THP-1 cells. After 24 h of incubation, cells were exposed to 100 μg/ml CML-HSA or HSA for 1 h before determinaton of luciferase activity. Results shown were normalized to the HSA control. *C*: Cells transfected with empty vector, wild-type (WT), or mutant (365t) RAGE and treated for 4 h with 100 μg/ml HSA, 100 μg/ml CML-HSA, or 10 ng/ml recombinant human TNF-α. We incubated 5 μg nuclear extract with radiolabeled double-stranded oligonucleotides containing the c-*myc* NF-κB binding site in the presence or absence of excess unlabeled probe (competitor). The data represent means ± SE of triplicate determinations in three separate experiments (P* < 0.05).**

binding to the radiolabeled oligonucleotide containing the c-*myc* NF-κB binding site (Fig. 1*C*). Specificity was confirmed by demonstrating that inclusion of 10-fold molar excess of unlabeled competitor probe prevented the appearance of specific (double arrows), but not nonspecific, DNA binding (single arrow). Unmodified HSA treatment had no effect on DNA binding over that observed in untreated extracts.

CML-HSA–mediated NF-κB transcriptional activation requires RAGE. To evaluate the role of RAGE in

Downloaded from http://diabetesjournals.org/diabetes/article-pdf/50/6/1495/654502/1495.pdf by guest on 04 December 2023

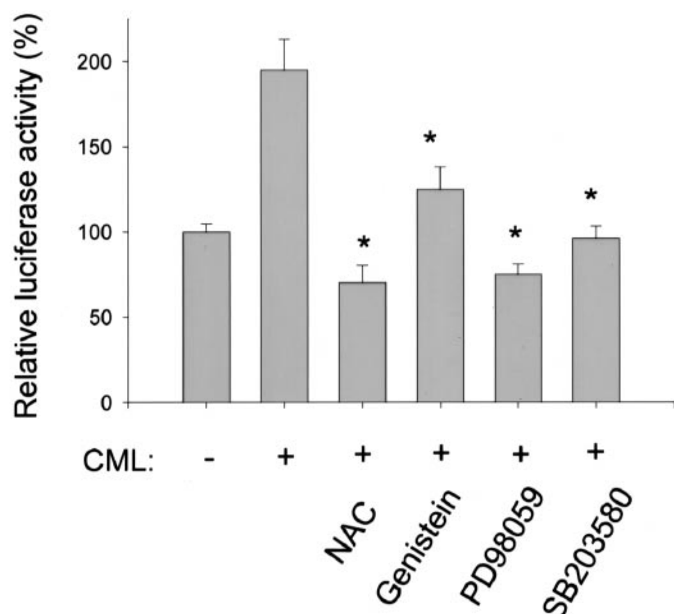

FIG. 3. Effects of N-acetyl-L-cysteine, genistein, PD98059, and SB203580 on NF-κB stimulation by CML-HSA. THP-1 cells transfected with the NF-κB reporter were preincubated with the antioxidant N-acetyl-L-cysteine (NAC, 500 μmol/l), a tyrosine kinase inhibitor genistein (100 μmol/l), an MEK-1 inhibitor (PD98059, 50 μmol/l), or a p38 inhibitor (SB203580, 10 μmol/l) at 37°C for 30 min. The cells were then exposed to 100 μg/ml CML-HSA for another 1 h and lysates were assayed for luciferase activity. NF-κB reporter activity with HSA treatment was defined as 100%. All values represent the means ± SE of at least three independent experiments (*P < 0.05).

CML-HSA–mediated NF-κB transcriptional activation, we prepared synthetic peptides based on sequences derived from the RAGE extracellular domain that have high probability of solvent accessibility. A 17–amino acid peptide encompassing residues 102–118 of RAGE neutralized CML-HSA activity in a dose-dependent manner such that a 20-fold molar excess effectively eliminated the NF-κB response (Fig. 2*A*). Peptides corresponding to amino acids 39–56 and amino acids 67–82 (both predicted to have a high probability of solvent accessibility) had no detectable effect (data not shown). Mouse antiserum to sRAGE also blocked the CML-HSA–induced NF-κB response in a dose-dependent manner (Fig. 2*A*).

To more clearly define the role of RAGE in CML-HSA signaling to NF-κB, we generated two RAGE cytoplasmic domain truncation mutants: RAGE-365t lacks the whole intracellular domain, whereas RAGE-372t retains a small nonconserved portion of the cytoplasmic tail. Both mutants and wild-type RAGE were individually coexpressed with the NF-κB reporter. In contrast to full-length (wild-type) RAGE, the mutants blocked the NF-κB response to CML-HSA (Fig. 2*B*). Similar results were seen when changes in NF-κB were measured by DNA binding activity (Fig. 2*C*). THP-1 cells were transfected with an empty vector (pcDNA3.1), wild-type RAGE, or the RAGE-365t. Both control and wild-type RAGE–transfected cells showed no increase in basal NF-κB DNA binding but exhibited a large increase after incubation with CML-HSA. RAGE-365t decreased the response to CML-HSA. Together, these results demonstrate that the intracellular domain of RAGE is required for CML-HSA–induced signaling to NF-κB and that expression of a RAGE in which this domain has been removed acts to block endogenous RAGE signaling in a trans-dominant manner. RAGE specificity was demonstrated by the inability of the RAGE mutant, the peptide, or RAGE antiserum to block a fourfold increase in luciferase activity induced by TNF-α (data not shown).

Involvement of reactive oxygen species, protein tyrosine kinase, and the MAPK family in CML-HSA–mediated NF-κB transcriptional activation. We next examined the effect of selective inhibitors of potentially relevant signaling molecules impinging on the reporter response. Cells transfected with the NF-κB reporter were pretreated for 30 min with each compound before stimulation with CML-HSA. As shown in Fig. 3, the antioxidant NAC; the MEK1 (an upstream kinase for ERK1/2) inhibitor, PD98059; and the p38 inhibitor SB203580 completely blocked CML-HSA–induced NF-κB activation. Similarly, genistein, the protein tyrosine kinase (PTK) inhibitor, resulted in a partial but significant reduction (~35%) in reporter activation. Together, these results suggest a role for reactive oxygen species, PTK, and MAPK in the signaling from RAGE to NF-κB.

CML-HSA induces tyrosine phosphorylation. Tyrosine phosphorylation is a crucial event that occurs rapidly and at a very early stage to propagate initial signals after activation of many receptors. Since genistein diminished NF-κβ activation by CML-HSA, we evaluated more directly the tyrosine phosphorylation profile after CML-HSA exposure. Stimulation of THP-1 cells with CML-HSA caused rapid phosphorylation (<10 min) on tyrosine residues of several proteins. Prominent phosphotyrosine polypeptides migrated at 75, 85, and 125 kDa (Fig. 4). Interestingly, the induced phosphotyrosine signals on these bands were abolished after 10 min and reappeared 60 min after treatment.

Activation of MAPK family members in response to CML-HSA treatment. The results shown in Fig. 3 suggest that CML-HSA–mediated signaling to NF-κB involves the MAPK family. To determine which MAPK was involved,

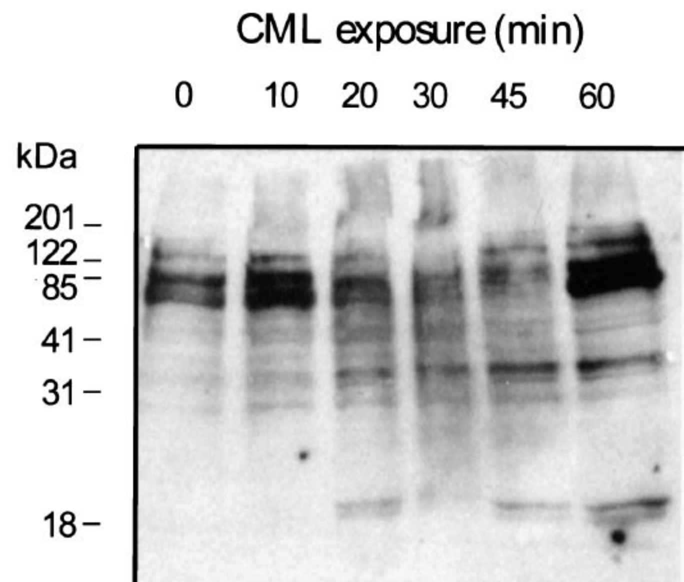

FIG. 4. Tyrosine phosphorylation profile in response to CML-HSA exposure. THP-1 cells were exposed to 100 μg/ml CML-HSA for the indicated times, cell extracts were analyzed by SDS-PAGE, and tyrosine-phosphorylated proteins were detected by blotting with an antiphosphotyrosine antibody. Results shown are representative of three independent experiments.

Downloaded from http://diabetesjournals.org/diabetes/article-pdf/50/6/1495/654502/1495.pdf by guest on 04 December 2023

we examined MAPK activation by Western blotting using antibodies specific to the active forms of the kinases. As shown in Fig. 5*A*, stimulation of THP-1 monocytes with CML-HSA enhanced ERK1/2 MAPK activities approximately twofold over basal levels. CML-HSA–mediated ERK activity peaked at 20 min and returned to basal levels by 45 min posttreatment. Moreover, incubation of cells with PD98059 for 30 min before CML-HSA stimulation resulted in complete inhibition of ERK1/2 activation, whereas addition of the p38 inhibitor SB203580 had no detectable effect.

p38 Kinase, another member of the MAPK family, also responded to CML-HSA treatment, as its activity was stimulated 1.3- to 2.1-fold between 5 and 30 min, with maximal kinase activity at 20 min after CML-HSA exposure (Fig. 5*B*). Like ERKs, p38 activity returned to basal levels 45 min after treatment. SB203580, the selective inhibitor of p38, blocked >80% of the p38 activation. PD98059 had no detectable effect. No changes were observed in the levels of JNK activation after CML-HSA stimulation (Fig. 5*C*). Concentrations of PD98059 and SB203580 that effectively blocked the NF-κB reporter response did not affect JNK activity.

CML-HSA–induced NF-κB transcriptional activation requires p38 MAPK. To establish a direct role for p38 MAPK in RAGE signaling leading to NF-κB transcriptional activation, THP-1 cells were transfected with the NF-κB reporter and an expression plasmid directing the synthesis of a dominant-negative form of p38. Overexpression of the kinase-dead p38 mutant completely blocked CML-HSA–mediated NF-κB activation, as did expression of an IκB mutant resistant to phosphorylation-dependent degradation (Fig. 6*A*). To further verify that the expressed p38 mutant competes efficiently with the endogenous wild-type kinase, we also measured the p38 kinase activity from empty vector-transfected and p38 mutant–transfected cells. In vitro kinase assays were performed using the transcription factor ATF-2, a downstream target of p38, as a substrate. Although total p38 protein levels were elevated by expressing the mutant (Fig. 6*B*, left panel), the p38 mutant–containing lysate had much less kinase activity compared with the empty vector–transfected control (Fig. 6*B*, right panel).

CML-HSA–induced monocytic cytokine release requires p38 MAPK and NF-κB. Since it is well established that NF-κB mediates proinflammatory responses by regulating the expression of a number of cytokines (38,39), and since CML-HSA induced p38-dependent NF-κB activation in THP-1 monocytes, we further investigated the role of p38 MAPK and NF-κB in CML-HSA–induced cytokine production. Mock-, p38-, or IκB mutant–transfected THP-1 cells were exposed to CML-HSA for 24 h, and secreted cytokines were measured. Table 1 shows that CML-HSA treatment induced a robust secretion of TNF-α and MCP-1 (~12- and 6-fold, respectively). IL-1β production was less dramatic but still increased ~3.5-fold by 24 h. Expression of the p38 dominant-negative mutant or the IκB mutant significantly reduced the CML-HSA–induced secretion of these cytokines, indicating that p38 MAPK and NF-κB are both required in the signaling pathway from RAGE to cytokine production. To strengthen and extend this observation, similar experiments were performed in peripheral blood-derived monocytes. As shown in Table 2, CML-HSA induced an approximately fourfold increase in TNF-α in primary monocytes, a response that was blocked by SB203580 and PD98059.

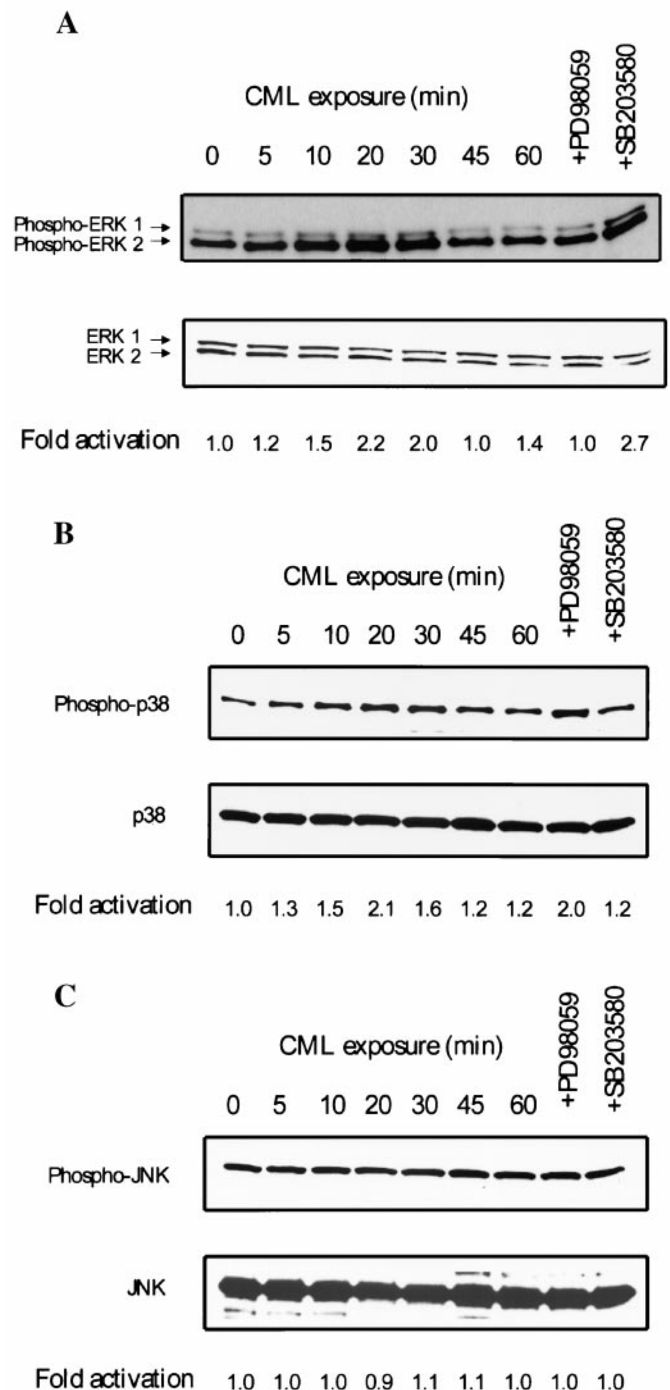

FIG. 5. CML-HSA treatment activates MAPK family members ERK1/2 and p38 but not JNK. Samples were taken at the indicated times after 100 μg/ml CML-HSA exposure and subjected to SDS-PAGE and Western blotting analysis. Upper panels: probed with an antibody that specifically recognizes the phosphorylated forms. Lower panels: the same membrane was stripped and reprobed with a pan antibody, showing equal protein loading of all lanes. *A*: ERK1/2; *B*: p38; and *C*: JNK. To test the effect of PD98059 and SB203580, cells were pretreated with either inhibitor for 30 min, followed by CML-HSA exposure for another 20 min, a time point at which the peak activation was seen. Results shown are representative of three independent experiments. Densitometric analysis for kinase activation by CML-HSA compared with the basal level (time 0, set as 1.0) is indicated.

Downloaded from http://diabetesjournals.org/diabetes/article-pdf/50/6/1495/654502/1495.pdf by guest on 04 December 2023

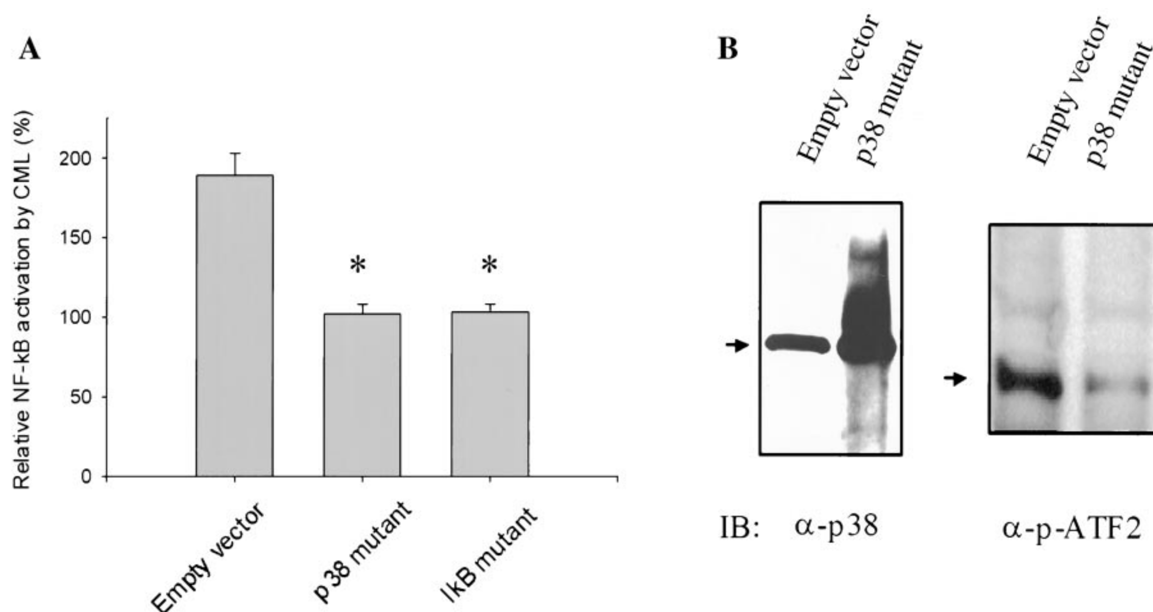

FIG. 6. Requirement of p38 MAPK in CML-HSA–induced NF-κB transcriptional activation. ***A*****: Cells were cotransfected with a kinase-dead p38 MAPK or an IκB dominant-negative mutant together with the reporter then treated for 1 h with 100 μg/ml CML-HSA or HSA, and results were normalized to the HSA treatment. Data are the means ± SE of at least three separate experiments (****P*** **< 0.05 compared with empty vector control).** ***B*****: Cell lysates from THP-1 cells that had been transfected with the p38 mutant or empty vector were analyzed by Western blotting using an anti-p38 antibody for protein level (left panel) or an anti-phospho–ATF-2 antibody for kinase activity after in vitro kinase reactions (right panel).**

DISCUSSION

The results of our experiments identify a signaling cascade in THP-1 monocytes in which CML-HSA binds RAGE, leading to phosphorylation of p38 MAPK and ERK1/2, causing increased DNA binding and transcriptional activation of NF-κB and secretion of proinflammatory cytokines. Although many AGEs have been identified, including pentosidine, methylglyoxal, pyralline, and imidizalone (1,3,4,9), to date, only CML has been reported to be an adduct on proteins that act as a ligand for RAGE (33). Our findings are consistent with previous observations that *1*) RAGE plays a role in chronic cellular activation and tissue injury by serving as a cell-surface receptor for the S100/calgranulin family of polypeptides that are released from activated inflammatory cells and accumulate at sites of chronic inflammation (6); *2*) AGE-induced increased endothelial cell tissue factor expression, a membrane-bound glycoprotein that initiates coagulation by its ability to bind factor VII/VIIa, is blocked by RAGE antisense (27); *3*) AGE-RAGE interaction induces cell-associated VCAM-1 expression (26); *4*) high–molecular weight hyaluronic acid blocks AGE-induced NF-κB activation and proinflammatory cytokine production in J774 mouse macrophages (40); and *5*) AGE adducts increase NF-κB DNA binding activity (24,30). Thus, although many studies have shown RAGE-induced NF-κB DNA binding activity, here we further show that this DNA binding leads to increased transcription of NF-κB target genes. These findings, together with the observations that NF-κB is a pleiotropic regulator of many "response-to-injury" genes and that the expression of this cell-surface receptor is upregulated in a number of diverse pathologies, suggest a central role for RAGE in the expression of proinflammatory and prothrombotic genes.

Our results demonstrate that the cytoplasmic domain of RAGE is required for CML adducts to activate NF-κB target gene transcription. These results are consistent with previous studies demonstrating that transient transfection of a cDNA-encoding RAGE lacking the cytoplasmic domain imparted a dominant-negative effect when the ligand

TABLE 1
CML-HSA–induced monocytic cytokine release requires p38 MAPK and NF-κB

Transfection	Treatment	Cytokine production (pg/ml) TNF-α	IL-1β	MCP-1
Mock	HSA	0.6 ± 0.2	0.2 ± 0.1	7.4 ± 0.2
Mock	CML-HSA	7.3 ± 0.3	0.7 ± 0.0	44.3 ± 0.5
p38 mutant	CML-HSA	2.5 ± 0.1*	0.1 ± 0.0*	20.7 ± 1.2*
IκB mutant	CML-HSA	2.2 ± 0.1*	0.1 ± 0.0*	25.8 ± 0.4*

Data are normalized by subtracting the background (TNF-α, 1.7 ± 0.2 pg/ml; IL-1β, 0.2 ± 0.1 pg/ml; MCP-1, 2.5 ± 0.6 pg/ml; mock, without treatment) and represent the means ± SE of three independent experiments. THP-1 cells were transfected and treated for 24 h as described, and culture media was collected for cytokine measurement. *$P < 0.05$ compared with mock, CML-HSA treatment.

TABLE 2
CML-HSA–induced TNF-α release in peripheral monocytes is sensitive to SB203580 and PD98059

Treatment	TNF-α production (pg/ml)
Sham	1.9 ± 0.1
HSA	2.8 ± 0.1
CML-HSA	11.0 ± 0.9
CML-HSA + SB203580	3.9 ± 0.4*
CML-HSA + PD98059	2.2 ± 0.3*

Data are the means ± SE of three independent experiments. Peripheral monocytes were treated for 24 h as described, and culture media was collected for TNF-α measurement by ELISA. *$P < 0.05$ compared with CML-HSA treatment.

Downloaded from http://diabetesjournals.org/diabetes/article-pdf/50/6/1495/654502/1495.pdf by guest on 04 December 2023

was CML-ovalbumin (33) or S100B (a member of the S100/calgranulin family) (6). A dominant-negative effect of the RAGE cytoplasmic tail also was reported on neurite outgrowth and NF-κB activation in N18 neuroblastoma and C6 glioma cells in response to AGE-modified bovine serum albumin and amphoterin (41).

Although the conserved cytoplasmic domain of RAGE is required for CML-HSA to activate NF-κB, only some of the signaling intermediates in the path from RAGE to the nucleus have been demonstrated. Thus, oxidant stress (24), PTK (42), p21Ras, and ERK1/2 MAPK (30) are involved in the AGE-mediated signaling cascade. In addition, it has been suggested that more than one parallel pathway can be activated simultaneously by the cytoplasmic domain of RAGE (41). In that study, it was demonstrated that Rac and Cdc42, the Rho family small GTPases, were responsible for RAGE-mediated neurite outgrowth induced by amphoterin, but not the simultaneous activation of NF-κB–dependent transcription, which was dependent on Ras-MAPK pathway. It is noteworthy that CML-HSA ligation of RAGE induced acute tyrosine phosphorylation followed by either dephosphorylation or degradation. For many transmembrane immunoglobulin-class receptors, signaling is initiated by ligand-induced aggregation that activates receptor-coupled tyrosine kinases (43,44). In most studies of mammalian receptors that signal by coupling to tyrosine kinase activation or that contain intrinsic tyrosine kinase activity, the earliest obligate intracellular event after ligand engagement is tyrosine phosphorylation (45,46). Although our results indicate that tyrosine phosphorylation plays an important role in RAGE signaling, no consensus kinase motif has been identified in the RAGE intracellular domain. Consequently, RAGE probably couples to a tyrosine kinase(s), directly or indirectly, to mediate tyrosine phosphorylation. Currently, intracellular proteins capable of binding to the RAGE cytoplasmic domain remain unknown.

A wide variety of extracellular signals regulate phosphorylation-dependent activation of MAPK family members that subsequently modulate transcriptional responses altering cellular function in normal and pathological settings. Although there is considerable cross-talk within these signaling cascades, some generalities have emerged regarding the specific types of information that are processed through the three MAPK family members. Thus, ERK typically mediates cell proliferation in response to growth factors, whereas p38 and JNK respond to cytokines and cellular stress inducers. Previously, RAGE ligands have been reported to activate ERK in arterial smooth muscle cells (30,47), rat pheochromocytoma PC12 cells (30), and renal tubulus cells in culture (48), indicating that this pathway is common across a variety of cell types. Our results implicate both ERK and p38 as key intermediates in CML-HSA activation of RAGE signaling leading to NF-κB–mediated target gene expression in a human monocytic cell line. The specificity of these responses is indicated by the lack of activation of JNK, the third MAPK family member. Additional specificity is evident since p38δ is not inhibited by SB203580, suggesting that other p38 isoforms must mediate the response to CML-HSA (49). These observations on p38 appear not to be unique to the AGE ligand used, CML-HSA, since amphoterin-induced RAGE signaling in C6 glioma cells activated p38 as well as p44/p42 (ERK) and stress-activated protein kinase/JNK MAPKs (50). Indeed, the extent of induction for ERK1/2 and p38 was comparable in both studies. Our inability to detect JNK activation in response to CML-HSA may be due to differences in cell types (THP-1 monocytes versus C6 glioma), exposure times (10–60 vs. 90 min), and ligand used (CML-HSA versus amphoterin), which may have different affinities for RAGE. Other recent reports have shown closely related results; CML-HSA increased NF-κB DNA binding through RAGE (33), and glycated serum albumin stimulated ERK activity and NF-κB DNA binding (30), but unfortunately, p38 was not evaluated in these studies.

Mechanisms that couple activation of MAPK to NF-κB target gene induction are complex. It is particularly important to note that NF-κB DNA binding activity is necessary, but not sufficient, for transcription, as shown in several reports and reviews (51). For example, IκB degradation and NF-κB DNA binding were insufficient for TNF- and IL-1β–induced NF-κB–dependent transcription (52). In addition, inhibition of TNF-induced p38 activation blocked NF-κB–dependent gene expression without decreasing DNA binding activity (53), leading to speculation that these intermediates converge at a more distal point. A subsequent report further delineated a mechanism wherein p38 phosphorylated the TATA-binding protein TFIID, increasing its binding to the p65 subunit of NF-κB (54), stabilizing the transcription complex and mediating gene expression. This mechanism was further supported by observations that inhibitors of p38 and ERKs cooperatively regulated the transactivation potential of the p65 subunit (55). Thus, increased DNA binding activity shown here and by others is only an intermediate readout of RAGE signaling and illustrates the importance of analyzing target gene expression, as we report here, for secretion of the cytokines IL-1β, TNF-α, and MCP-1. Finally, our observations that both p38 and ERK mediate RAGE-dependent NF-κB target gene induction suggest that RAGE may be a pleiotropic integrator of AGEs that signal both growth factor–like proliferative responses as well as cytokine-like proinflammatory responses.

The present studies demonstrate that p38 activation is necessary for CML-HSA–mediated RAGE-dependent NF-κB activation, induction of target gene expression, and secretion of proinflammatory cytokines from monocytes. The identification of a RAGE signaling axis involving p38 extends our understanding of AGE-induced cellular dysfunction and provides a possible mechanism for p38 involvement in inflammation, arthritis, septic shock, and myocardial dysfunction after ischemia (56–59). Furthermore, since AGEs—particularly CML adducts—are prevalent in diseases such as diabetes, renal failure, chronic inflammation, and Alzheimer's disease (6,32,33,60), our findings may provide another pathophysiologically relevant mechanism linked to these disorders. Understanding the integrative aspects of RAGE in the diverse pathologies of AGEs provides a key challenge for future studies.

ACKNOWLEDGMENTS

We thank Dr. Kaijun Ren (Chemistry Department at Texas Biotechnology Corporation) for the synthesis of peptides used in the RAGE inhibition studies, and Drs. Roger Davis (Howard Hughes Medical Institute at the University of

Downloaded from http://diabetesjournals.org/diabetes/article-pdf/50/6/1495/654502/1495.pdf by guest on 04 December 2023

Massachusetts Medical Center, Worcester, MA) and Chung Y. Hsu (Washington University School of Medicine, St. Louis, MO) for the p38 kinase–dead and IκB dominant-negative mutants, respectively.

REFERENCES

1. Brownlee M: Advanced protein glycosylation in diabetes and aging. *Annu Rev Med* 46:223–234, 1995
2. Bucala R, Cerami A: Advanced glycosylation: chemistry, biology, and implications for diabetes and aging. *Adv Pharmacol* 23:1–34, 1992
3. Vlassara H, Bucala R, Striker L: Pathogenic effects of advanced glycosylation: biochemical, biologic, and clinical implications for diabetes and aging. *Lab Invest* 70:138–151, 1994
4. Thornalley PJ: Cell activation by glycated proteins: AGE receptors, receptor recognition factors and functional classification of AGEs. *Cell Mol Biol* 44:1013–1023, 1998
5. Schmidt AM, Yan SD, Wautier JL, Stern D: Activation of receptor for advanced glycation end products: a mechanism for chronic vascular dysfunction in diabetic vasculopathy and atherosclerosis. *Circ Res* 84:489–497, 1999
6. Hofmann MA, Drury S, Fu C, Qu W, Taguchi A, Lu Y, Avila C, Kambham N, Bierhaus A, Nawroth P, Neurath MF, Slattery T, Beach D, McClary J, Nagashima M, Morser J, Stern D, Schmidt AM: RAGE mediates a novel proinflammatory axis: a central cell surface receptor for S100/calgranulin polypeptides. *Cell* 97:889–901, 1999
7. Yan SD, Chen X, Fu J, Chen M, Zhu H, Roher A, Slattery T, Zhao L, Nagashima M, Morser J, Migheli A, Nawroth P, Stern D, Schmidt AM: RAGE and amyloid-beta peptide neurotoxicity in Alzheimer's disease. *Nature* 382:685–691, 1996
8. Niwa T, Sato M, Katsuzaki T, Tomoo T, Miyazaki T, Tatemichi N, Takei Y, Kondo T: Amyloid beta 2-microglobulin is modified with N epsilon-(carboxymethyl)lysine in dialysis-related amyloidosis. *Kidney Int* 50:1303–1309, 1996
9. Vlassara H: Recent progress in advanced glycation end products and diabetic complications. *Diabetes* 46 (Suppl. 2):S19–S25, 1997
10. Hammes HP, Martin S, Federlin K, Geisen K, Brownlee M: Aminoguanidine treatment inhibits the development of experimental diabetic retinopathy. *Proc Natl Acad Sci U S A* 88:11555–11558, 1991
11. Edelstein D, Brownlee M: Aminoguanidine ameliorates albuminuria in diabetic hypertensive rats. *Diabetologia* 35:96–97, 1992
12. Schmidt AM, Vianna M, Gerlach M, Brett J, Ryan J, Kao J, Esposito C, Hegarty H, Hurley W, Clauss M, Wand F, Pan Y-C, Tsang TC, Stern D: Isolation and characterization of two binding proteins for advanced glycosylation end products from bovine lung which are present on the endothelial cell surface. *J Biol Chem* 267:14987–14997, 1992
13. Yang Z, Makita Z, Horii Y, Brunelle S, Cerami A, Sehajpal P, Suthanthiran M, Vlassara H: Two novel rat liver membrane proteins that bind advanced glycosylation endproducts: relationship to macrophage receptor for glucose-modified proteins. *J Exp Med* 174:515–524, 1991
14. Li YM, Mitsuhashi T, Wojciechowicz D, Shimizu N, Li J, Stitt A, He C, Banerjee D, Vlassara H: Molecular identity and cellular distribution of advanced glycation endproduct receptors: relationship of p60 to OST-48 and p90 to 80K-H membrane proteins. *Proc Natl Acad Sci U S A* 93:11047–11052, 1991
15. Vlassara H, Li YM, Imani F, Wojciechowicz D, Yang Z, Liu FT, Cerami A: Molecular identity and cellular distribution of advanced glycation endproduct receptors: relationship of p60 to OST-48 and p90 to 80K-H membrane proteins. *Mol Med* 1:634–646, 1995
16. Li YM, Tan AX, Vlassara H: Antibacterial activity of lysozyme and lactoferrin is inhibited by binding of advanced glycation-modified proteins to a conserved motif. *Nat Med* 1:1057–1061, 1995
17. Neeper M, Schmidt AM, Brett J, Yan SD, Wang F, Pan YC, Elliston K, Stern D, Shaw A: Cloning and expression of a cell surface receptor for advanced glycosylation end products of proteins. *J Biol Chem* 267:14998–15004, 1992
18. Brett J, Schmidt AM, Yan SD, Zou YS, Weidman E, Pinsky D, Nowygrod R, Neeper M, Przysiecki C, Shaw A: Survey of the distribution of a newly characterized receptor for advanced glycation end products in tissues. *Am J Pathol* 143:1699–1712, 1993
19. Schmidt AM, Hori O, Brett J, Yan SD, Wautier JL, Stern D: Cellular receptors for advanced glycation end products: implications for induction of oxidant stress and cellular dysfunction in the pathogenesis of vascular lesions. *Arterioscler Thromb* 14:1521–1528, 1994
20. Schmidt AM, Yan SD, Stern DM: The dark side of glucose. *Nat Med* 1:1002–1004, 1995
21. Miyata T, Hori O, Zhang J, Yan SD, Ferran L, Iida Y, Schmidt AM: The receptor for advanced glycation end products (RAGE) is a central mediator of the interaction of AGE-β2 microglobulin with human mononuclear phagocytes via an oxidant-sensitive pathway: implications for the pathogenesis of dialysis-related amyloidosis. *J Clin Invest* 98:1088–1094, 1996
22. Wautier JL, Zoukourian C, Chappey O, Wautier MP, Guillausseau PJ, Cao R, Hori O, Stern D, Schmidt AM: Receptor-mediated endothelial cell dysfunction in diabetic vasculopathy: soluble receptor for advanced glycation end products blocks hyperpermeability in diabetic rats. *J Clin Invest* 97:238–243, 1996
23. Park L, Raman KG, Lee J, Lu Y, Ferran LJ Jr, Chow WS, Stern D, Schmidt AM: Suppression of accelerated diabetic atherosclerosis by the soluble receptor for advanced glycation endproducts. *Nat Med* 4:1025–1031, 1998
24. Yan SD, Schmidt AM, Anderson GM, Zhang J, Brett J, Zou YS, Pinsky D, Stern D: Enhanced cellular oxidant stress by the interaction of advanced glycation end products with their receptors/binding proteins. *J Biol Chem* 269:9889–9897, 1994
25. Lavrovsky Y, Schwartzman ML, Levere RD, Kappas A, Abraham NG: Identification of binding sites for transcription factors NF-κB and AP-2 in the promoter region of the human heme oxygenase 1 gene. *Proc Natl Acad Sci U S A* 91:5987–5991, 1994
26. Schmidt AM, Hori O, Chen JX, Li JF, Crandall J, Zhang J, Cao R, Yan SD, Brett J, Stern D: Advanced glycation endproducts interacting with their endothelial receptor induce expression of vascular cell adhesion molecule-1 (VCAM-1) in cultured human endothelial cells and in mice: a potential mechanism for the accelerated vasculopathy of diabetes. *J Clin Invest* 96:1395–1403, 1995
27. Bierhaus A, Illmer T, Kasper M, Luther T, Quehenberger P, Tritschler H, Wahl P, Ziegler R, Muller M, Nawroth PP: Advanced glycation end product (AGE)-mediated induction of tissue factor in cultured endothelial cells is dependent on RAGE. *Circulation* 96:2262–2271, 1997
28. Bierhaus A, Ziegler R, Nawroth PP: Molecular mechanisms of diabetic angiopathy: clues for innovative therapeutic interventions. *Horm Res* 50 (Suppl. 1):1–5, 1998
29. Li J, Schmidt AM: Characterization and functional analysis of the promoter of RAGE, the receptor for advanced glycation end products. *J Biol Chem* 272:16498–16506, 1997
30. Lander HM, Tauras JM, Ogiste JS, Hori O, Moss RA, Schmidt AM: Activation of the receptor for advanced glycation end products triggers a p21(ras)-dependent mitogen-activated protein kinase pathway regulated by oxidant stress. *J Biol Chem* 272:17810–17814, 1997
31. Horie K, Miyata T, Maeda K, Miyata S, Sugiyama S, Sakai H, Strihou CY, Monnier VM, Witztum JL, Kurokawa K: Immunohistochemical colocalization of glycoxidation products and lipid peroxidation products in diabetic renal glomerular lesions: implication for glycoxidative stress in the pathogenesis of diabetic nephropathy. *J Clin Invest* 100:2995–3004, 1997
32. Schleicher ED, Wagner E, Nerlich AG: Increased accumulation of the glycoxidation product N(epsilon)-(carboxymethyl)lysine in human tissues in diabetes and aging. *J Clin Invest* 99:457–468, 1997
33. Kislinger T, Fu C, Huber B, Qu W, Taguchi A, Du-Yan S, Hofmann M, Yan SF, Pischetsrieder M, Stern D, Schmidt AM: N(epsilon)-(carboxymethyl) lysine adducts of proteins are ligands for receptor for advanced glycation end products that activate cell signaling pathways and modulate gene expression. *J Biol Chem* 274:31740–31749, 1999
34. Ikeda K, Higashi T, Sano H, Jinnouchi Y, Yoshida M, Araki T, Ueda S, Horiuchi S: N (epsilon)-(carboxymethyl)lysine protein adduct is a major immunological epitope in proteins modified with advanced glycation end products of the Maillard reaction. *Biochemistry* 35:8075–8083, 1996
35. Kanof ME, Smith PD, Zola H: Preparation of human mononuclear cell populations and subpopulations. In *Current Protocols in Immunology*. Coligan JE, Kruisbeek AM, Margulies DH, Shevach EM, Strober W, Eds. New York, Greene Publishing and John Wiley & Sons, p. 7.1.1–7.1.7, 1996
36. Shirakawa F, Saito K, Bonagura CA, Galson DL, Fenton MJ, Webb AC, Auron PE: The human prointerleukin 1 beta gene requires DNA sequences both proximal and distal to the transcription start site for tissue-specific induction. *Mol Cell Biol* 13:1332–1344, 1993
37. Schreiber E, Matthias P, Muller MM, Schaffner W: Rapid detection of octamer binding proteins with "mini-extracts," prepared from a small number of cells. *EMBO J* 7:4221–4229, 1988
38. Beg AA, Baltimore D: An essential role for NF-κB in preventing TNF-α–induced cell death. *Science* 274:782–784, 1996
39. Miagkov AV, Kovalenko DV, Brown CE, Didsbury JR, Cogswell JP, Stimpson SA, Baldwin AS, Makarov SS: NF-κB activation provides the potential link between inflammation and hyperplasia in the arthritic joint. *Proc Natl Acad Sci U S A* 95:13859–13864, 1998
40. Neumann A, Schinzel R, Palm D, Riederer P, Munch G: High molecular

Downloaded from http://diabetesjournals.org/diabetes/article-pdf/50/6/1495/654502/1495.pdf by guest on 04 December 2023

weight hyaluronic acid inhibits advanced glycation endproduct-induced NF-κB activation and cytokine expression. *FEBS Lett* 453:283–287, 1999
41. Huttunen HJ, Fages C, Rauvala H: Receptor for advanced glycation end products (RAGE)-mediated neurite outgrowth and activation of NF-κB require the cytoplasmic domain of the receptor but different downstream signaling pathways. *J Biol Chem* 274:19919–19924, 1999
42. Khechai F, Ollivier V, Bridey F, Amar M, Hakim J, de Prost D: Effect of advanced glycation end product–modified albumin on tissue factor expression by monocytes: role of oxidant stress and protein tyrosine kinase activation. *Arterioscler Thromb Vasc Biol* 17:2885–2890, 1997
43. Santana C, Noris G, Espinoza B, Ortega E: Protein tyrosine phosphorylation in leukocyte activation through receptors for IgG. *J Leukoc Biol* 60:433–440, 1996
44. Sanchez-Mejorada G, Rosales C: Fcγ receptor-mediated mitogen-activated protein kinase activation in monocytes is independent of Ras. *J Biol Chem* 273:27610–27619, 1998
45. Fukazawa T, Miyake S, Band V, Band H: Tyrosine phosphorylation of Cbl upon epidermal growth factor (EGF) stimulation and its association with EGF receptor and downstream signaling proteins. *J Biol Chem* 271:14554–14559, 1996
46. Lipson KE, Pang L, Huber LJ, Chen H, Tsai JM, Hirth P, Gazit A, Levitzki A, McMahon G: Inhibition of platelet-derived growth factor and epidermal growth factor receptor signaling events after treatment of cells with specific synthetic inhibitors of tyrosine kinase phosphorylation. *J Pharmacol Exp Ther* 285:844–852, 1998
47. Satoh H, Togo M, Hara M, Miyata T, Han K, Maekawa H, Ohno M, Hashimoto Y, Kurokawa K, Watanabe T: Advanced glycation endproducts stimulate mitogen-activated protein kinase and proliferation in rabbit vascular smooth muscle cells. *Biochem Biophys Res Commun* 239:111–115, 1997
48. Simm A, Munch G, Seif F, Schenk O, Heidland A, Richter H, Vamvakas S, Schinzel R: Advanced glycation endproducts stimulate the MAP-kinase pathway in tubulus cell line LLC-PK1. *FEBS Lett* 410:481–484, 1997
49. Jiang Y, Gram H, Zhao M, New L, Gu H, Feng L, DiPadova F, Ulevitch RJ, Han J: Characterization of the structure and function of the fourth member of p38 group mitogen-activated protein kinases, p38δ. *J Biol Chem* 272:30122–30128, 1997
50. Taguchi A, Blood DC, del Toro G, Canet A, Lee DC, Qu W, Tanji N, Lu Y, Lalla E, Fu C, Hofmann MA, Kislinger T, Ingram M, Lu A, Tanaka H, Hori O, Ogawa S, Stern DM, Schmidt AM: Blockade of RAGE-amphoterin signalling suppresses tumour growth and metastases. *Nature* 405:354–360, 2000
51. Li N, Karin M: Is NF-κB the sensor of oxidative stress? *FASEB J* 13:1137–1143, 1999
52. Bergmann M, Hart L, Lindsay M, Barnes PJ, Newton R: Iκ-Bα degradation and nuclear factor-κB DNA binding are insufficient for interleukin-1β and tumor necrosis factor-α–induced κB-dependent transcription: requirement for an additional activation pathway. *J Biol Chem* 273:6607–6610, 1998
53. Wesselborg S, Bauer MKA, Vogt M, Schmitz ML, Schulze-Osthoff K: Activation of transcription factor NF-κB and p38 mitogen-activated protein kinase is mediated by distinct and separate stress effector pathways. *J Biol Chem* 272:12422–12429, 1997
54. Carter AB, Knudtson KL, Monick MM, Hunninghake GW: The p38 mitogen-activated protein kinase is required for NF-κB–dependent gene expression: the role of TATA-binding protein (TBP). *J Biol Chem* 274:30858–30863, 1999
55. Vanden-Berghe W, Plaisance S, Boone E, De Bosscher K, Schmitz ML, Fiers W, Nishida E, Matsumoto K: P38 and extracellular signal-regulated kinase mitogen-activated protein kinase pathways are required for nuclear factor-κB p65 transactivation mediated by tumor necrosis factor. *Science* 270:2008–2011, 1995
56. Lee JC, Kassis S, Kumar S, Badger A, Adams JL: P38 mitogen-activated protein kinase inhibitors: mechanisms and therapeutic potentials. *Pharmacol Ther* 82:389–397, 1999
57. Herlaar E, Brown Z: p38 MAPK signalling cascades in inflammatory disease. *Mol Med Today* 5:439–447, 1999
58. Salituro FG, Germann UA, Wilson KP, Bemis GW, Fox T, Su MS: Inhibitors of p38 MAP kinase: therapeutic intervention in cytokine-mediated diseases. *Curr Med Chem* 6:807–823, 1999
59. Cain BS, Meldrum DR, Meng X, Dinarello CA, Shames BD, Banerjee A, Harken AH: p38 MAPK inhibition decreases TNF-α production and enhances postischemic human myocardial function. *J Surg Res* 83:7–12, 1999
60. Degenhardt TP, Grass L, Reddy S, Thorpe SR, Diamandis EP, Baynes JW: Technical note: the serum concentration of the advanced glycation end-product N epsilon-(carboxymethyl)lysine is increased in uremia. *Kidney Int* 52:1064–1067, 1997

Downloaded from http://diabetesjournals.org/diabetes/article-pdf/50/6/1495/654502/1495.pdf by guest on 04 December 2023